Mode lock-in and friction modelling

R. Allgaier,[1] L. Gaul,[2] W. Keiper,[1] K. Willner[2]
[1] *Robert Bosch GmbH, Dept.: FV/FLP, 70049 Stuttgart*
Email: Ralph.Allgaier@de.bosch.com
Winfried.Keiper@de.bosch.com
[2] *University of Stuttgart, Institute A of Mechanics, 70550 Stuttgart*
Email: L.Gaul@mecha.uni-stuttgart.de
K.Willner@mecha.uni-stuttgart.de

Abstract

In this paper the phenomenon of "mode lock-in" is investigated, which occurs in structures where vibrations are excited by frictional forces. In general "mode lock-in" is defined as the process by which modes of sub-structures couple with each other. A resonant response of the assembly (mode lock-in) is the result of the latter.
For studying this effect an experimental pin-disc set-up was built in collaboration with Akay [1] and a corresponding FEM model was generated. The rotational speed of the disc, beam length, and the two parameters "normal force" and "angle of attack between pin and disc" can be varied with the pin-disc apparatus. The linear FE model is updated by EMA (Experimental Modal Analysis).
A number of different contact descriptions, partly based on surface roughness and material constants of the bodies in contact introduced by Willner and Gaul [4] was formulated and introduced, as user-defined subroutines, into a commercial FE solver. The friction couple considered consists of aluminium/aluminium. The time-marching solutions of the FE model were checked for system resonances and compared to the experimentally observed mode lock-in.
The primary objective of this investigation is to determine which friction model and which modelling details are necessary and sufficient to simulate mode lock-in.

1 Introduction

Friction-induced oscillations occur in many physical systems. A system of great practical importance is, e.g., the brake. Disc brakes can develop large sustained

oscillations which are heard as "brake squeal". At present, no comprehensive model for the many phenomena of brake squeal exists.
This paper presents a novel approach to the numerical modelling of brake squeal as a friction-induced oscillation. A highly simplified physical system is used: The pin-on-disc device. This apparatus has the advantage of reduced complexity:

- well-defined components and boundary conditions,
- well-defined confined contact area,
- simple friction couple.

The dynamics of the pin-on-disc device nevertheless has characteristic features of more complex systems:

- friction in the plane of the disc leads to large out-of-plane oscillations of the disc,
- modes of the components "lock" into new "assembly modes" when coupled through a friction interface.

The pin-on-disc device is therefore a well-suited test object for the development of numerical representations of contact laws.

2 Mode lock-in

The investigated system consists of two components (pin and disc) whose dynamics (natural frequencies and vibration modes) are well understood, when they are considered separately. The assembly, as coupled through a friction interface, has somewhat different system frequencies and modes. Non-linear friction coupling causes particular modes of the components to lock into one another. When mode lock-in takes place, a special base frequency with all of its harmonics can be observed in the resonant-like system response. For example, when the second mode of the free pin and the first mode of the free disc are almost equal in frequency, look-in occurs at almost exactly that frequency. The latter is a typical case of so called "classical" lock-in signature. From many measurements, e.g. reported by Akay [1] it is known, that mode lock-in has several characteristics. The second type of mode lock-in can be characterized by means of an "intermediate" lock-in response, that is the system locks into a frequency which lies in between eigenfrequencies of pin and disc. Another case is called "multiple" lock-in where the squeal spectrum contains not only a dominant frequency and its harmonics, but also side bands. Alternatively, dual base frequencies and all of their harmonics can be present.
In summary: Mode lock-in can occur at a natural frequency of the disc and all of their harmonics, but other more complicated responses having greater spectral content can also occur.

2.1 Mode lock-in test set-up

The mode lock-in test set-up consists of two subsystems, a rotating disc and a beam, as shown in Figure 1. The disc has a diameter of 358 mm and a thickness of 25 mm. By means of a DC motor and a belt pulley the relative sliding velocity can be varied in a range of 0.5 RPM to 95 RPM. The pin has a variable length

from 0 mm to 200 mm to vary its natural frequencies and a square cross section of 10 mm. The pin is clamped in a jaw-chuck, which is fixed on a guide plate, which travels on two linear bearings. Furthermore, the angle of attack between the vector normal to the disc and the neutral axis of the pin can be changed by rotating the fixing of the jaw-chuck on the guide plate. Pin and disc are in contact above the centre of the disc. The normal load on the pin is generated by weight (adjustable from 0.5 kg to 5 kg) which press the two subsystems together. The vibrations of the disc are measured by using a triax laser vibrometer. The vibrations of the pin are measured by means of a triax accelerometer. Noise generated by friction-induced vibrations is measured using a ¼"-microphon. All data are acquired and processed on a four-channel spectrum analyzer. All of the experiments are conducted with a direct aluminium to aluminium contact at the friction interface.

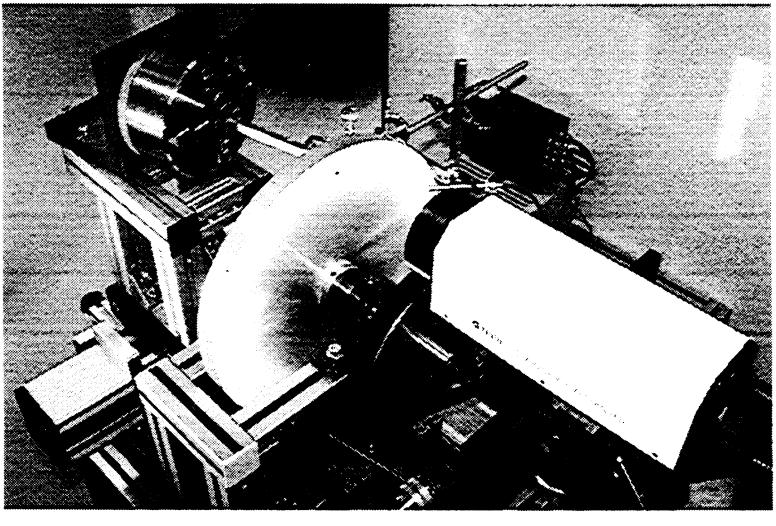

Figure 1. Experimental pin-disc set-up

2.2 FE model

The complete FE model used to simulate mode lock-in, and an enlarged detail, the contact area, are shown in Figure 1 and 2. The volumes of the pin-disc model are discretized using first-order hexahedron elements exclusively. From the number of nodes (3187) and the additional degress of freedom by contact, one obtains 10824 DOF's altogether. Rigid beams are fixed between the centre and the inner diameter of the disc. By rotating the centre nodes, a circular movement of the disc is generated. By means of restraints at the end of the pin, a movement of the pin in direction of the normal vector to the disc surface is forced. In order to bring both components of the friction couple into contact a force is applied at the end of the pin. The position of the pin relative to the disc is the same as described in the section of the experimental set-up.

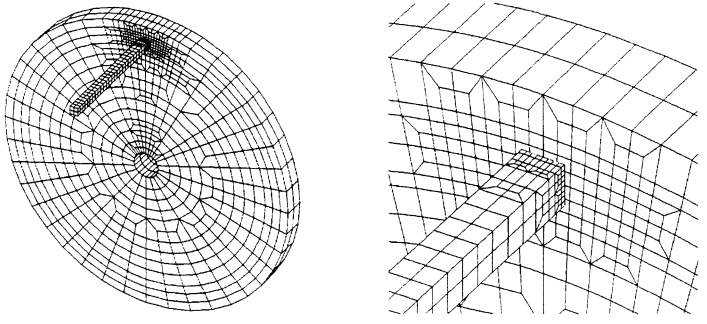

Figure 2. FE model pin-disc

2.2.1 FE model update

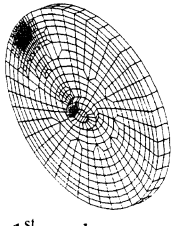

1st mode:
f_{1m} = 292 Hz
f_{1c} = 435 Hz

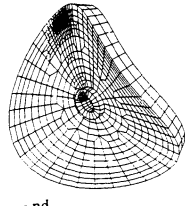

2nd mode:
f_{2m} = 1005 Hz
f_{2c} = 1020 Hz

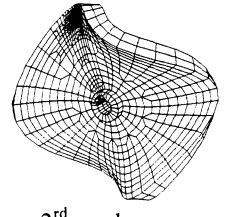

3rd mode:
f_{3m} = 2240 Hz
f_{3c} = 2247 Hz

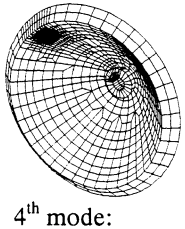

4th mode:
f_{4m} = 2437 Hz
f_{4c} = 2418 Hz

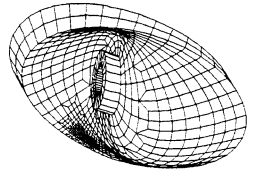

5th mode:
f_{5m} = 3648 Hz
f_{5c} = 3603 Hz

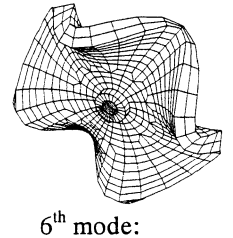

6th mode:
f_{6m} = 3819 Hz
f_{6c} = 3833 Hz

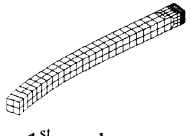

1st mode:
f_{1m} = 356 Hz
f_{1c} = 365 Hz

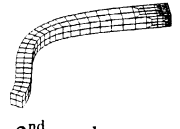

2nd mode:
f_{2m} = 2247 Hz
f_{3c} = 2250 Hz

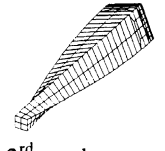

3rd mode:
f_{3m} = 4370 Hz
f_{3c} = 4308 Hz

Figure 3. Eigenfrequencies and mode shapes of disc and pin

For direct comparison of the results from simulation and experiment, it is necessary to update the dynamic behaviour of the FE model to the experimental set-up. As a first step, both pin and disc are updated in free/free boundary conditions using natural frequencies and mode shapes measured by EMA. Secondly, another EMA of the assembly is carried out. Using these data, the real acting boundary conditions are taken into account at the numerical model. The model update is made in a frequency range of 500 Hz to 5 kHz. Figure 3 shows the mode shapes in assembled condition, identified by means of EMA, and the comparison between measured (m) and calculated (c) natural frequencies as well.

3 Contact laws

In order to obtain realistic surface parameters for the simulation, a contact interface model [4] based on a statistical description of the surface roughness is used to derive a non-linear constitutive description for normal- and tangential contact.
The following assumptions are made:

- elastic contact of metallic surfaces
- isotropic surface roughness
- contact points do not interfere with each other
- surface parameters do not change with time
- dry friction

3.1 Normal contact

Using these assumptions, each local contact area can be described by Hertzian theory. The normal force K_i to compress a summit i with normalized curvature s in contact with a plane is given by

$$K_i(\eta) = \frac{4}{3} E \frac{1}{\sqrt{\sigma_k s}} (\zeta - \eta)^{\frac{3}{2}} \sigma^{\frac{3}{2}}, \tag{1}$$

with the normalized gap function η, Young's modulus E, root mean square value of the curvature σ_k, normalized height of the summit above a reference level ζ and the root mean square value of the height distribution of summits σ.

3.2 Tangential contact

The tangential load-displacement function is formulated under the assumption of a total contact radius a calculated by Hertzian theory and a constant shear yield strenght τ_{max} of the junction. The tangential force Q_i of an asperity i with the normalized relative tangential displacement υ is given by

$$Q_i(\upsilon, \eta) = \frac{\pi}{3} \tau_{\max} a^2 \left[\left(1 - \alpha^2\right) + 2 \frac{1 - \alpha^3}{\sqrt{1 - \alpha^2}} \right], \tag{2}$$

with the relative radius α between slip and stick areas.

3.3 Contact laws

For the implementation in a macroscopic model the relations have to be distributed on the apparent area of contact. This is done via a statistical model of the surface, which assumes that the distribution of heights is Gaussian. With the probability P for a summit with normalized curvature s and height ζ, the apparent normal contact pressure p of all summits above η is

$$p(\eta) = \frac{1}{h^2} \int_{\eta}^{\infty} \int_{0}^{\infty} K_i(\eta) P(\zeta, s) ds d\zeta \tag{3}$$

and the tangential contact stress is given by

$$\tau(\upsilon, \eta) = \frac{1}{h^2} \int_{\eta}^{\infty} \int_{0}^{\infty} Q_i(\upsilon, \eta) P(\zeta, s) ds d\zeta \,, \tag{4}$$

with resolution h of the surface roughness measurements.

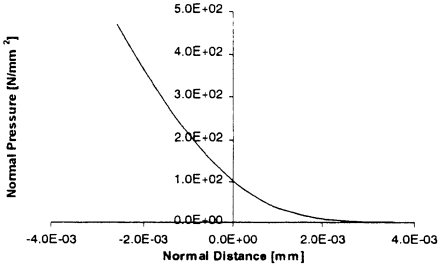

Figure 4. Normal pressure vs. normal distance

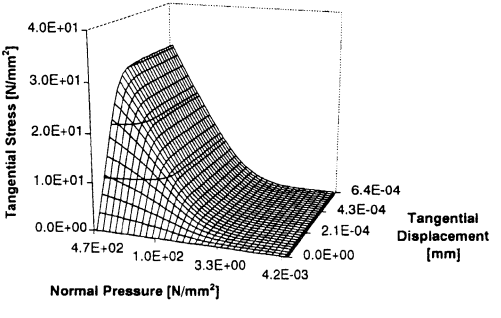

Figure 5. Tangential stress vs. normal pressure and tangential displacement

Figures 4 and 5 show the constitutive laws of the contact interface using the equations above and surface roughness data of both pin and disc measured by laser scanning profilometry with a resolution h of 1 μm. The material is aluminium and the material parameters are $E=70000\ N/mm^2$, Poison's ratio $\nu=0.33$ and $\tau_{max}=385\ N/mm^2$.

4 Contact description

The following section describes three different possibilities how to implement the friction relation, as in Figure 5, into a FE code. Furthermore, the importance of friction modelling details, such as tangential contact stiffness, maximum transmittable tangential contact stress (corresponding to a friction coefficient) and transition from micro- to macroslip as given by the friction law used in section 3 is investigated. Three models are implemented in a standard FE code by means of user subroutines.

Tangential contact virtual work for Penalty formulation is given by [3]

$$\delta W_{C,Pe} = \int_{\Gamma} \tau_i \, \delta\gamma_i \, d\Gamma \cdot \tag{5}$$

Tangential contact virtual work for Lagrange multiplier formulation is given by [2]

$$\delta W_{C,La} = \int_{\Gamma} (\tau_i \, \delta\gamma_i + \Delta\gamma_i \, \delta\tau_i) \, d\Gamma \cdot \tag{6}$$

Standard FE techniques (linearization, inkrementation) lead to contact stiffness and residual.

4.1 Evolution rule (Penalty)

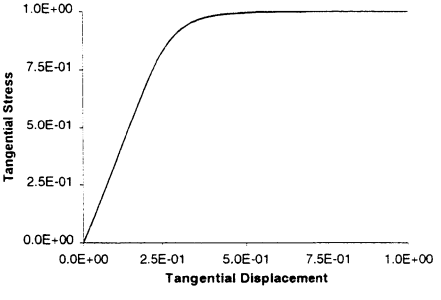

Figure 6. Tangential stress vs. tangential displacement at constant pressure using evolution rule

Tangential contact stiffness is represented by [4]

$$\partial\tau_i = c_t \left[1 - \frac{1}{2}\left(1 + \operatorname{sgn}(\partial\gamma_j \, \tau_j)\right) \left| \frac{\tau}{\tau_{\max}} \right|^m \right] \partial\gamma_i \,, \tag{7}$$

with pressure dependent parameters tangential contact stiffness $c_t(p)$, maximum transmittable tangential contact stress $\tau_{max}(p)$ and exponent $m(p)$ corresponding to Figure 5.

4.2 Elastic-sticking approach (Penalty)

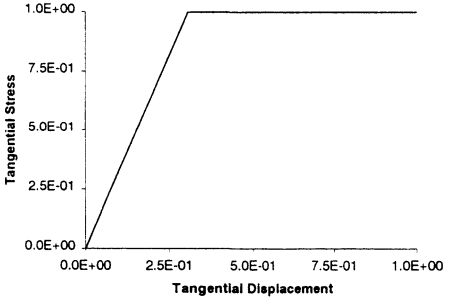

Figure 7. Tangential stress vs. tangential displacement at constant pressure using elastic-sticking approach

Tangential contact stiffness is given by [2]

$$\partial\tau_i = c_t\,\partial\gamma_i + \frac{\tau}{\tau_{\max}}(\mu + p\frac{\partial\mu}{\partial p})\partial p, \qquad \text{(sticking)} \qquad (8)$$

$$\partial\tau_i = \frac{\tau_{\max}}{\gamma}(\delta_{ij} - n_i n_j)\partial\gamma_j + n_i(\mu + p\frac{\partial\mu}{\partial p})\partial p, \qquad \text{(slipping)} \qquad (9)$$

with pressure dependent friction coefficient $\mu(p)$ according to Figure 5.

4.3 Rigid-sticking approach (Lagrange)

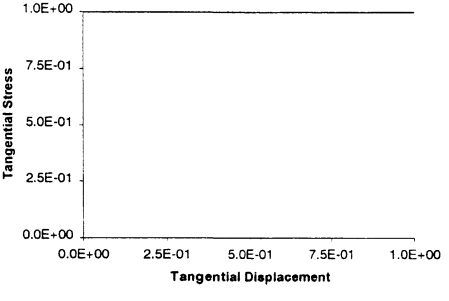

Figure 8. Tangential stress vs. tangential displacement at constant pressure using rigid-sticking approach

Tangential contact stiffness is represented by [2]

$$\partial\tau_i = \frac{\tau_{\max}}{\Delta\gamma}(\delta_{ij} - n_i n_j)\partial\gamma_i + n_i(\mu + p\frac{\partial\mu}{\partial p})\partial p\,. \qquad \text{(slipping)} \qquad (10)$$

From extensive numerical studies we obtained as first result, that the correct reproduction of tangential contact stiffness (reproduceable by evolution rule and elastic-sticking approach) and the steady transition from micro- to macroslip

(reproduceable by evolution rule only) has no importance in this case. No differences between the results for each approach could be found. Further investigations significantly showed, that the evolution rule (Penalty formulation) offers indeed the best approximation of the tangential load-displacement function (see Figure 5), however it has the worst convergence rate (sometimes it diverges) of all. Convergence problems occured especially under slipping conditions at 3D contact. This can be traced back to the missing unsymmetric terms of the tangential contact stiffness matrix, the derivative with respect to p [2]. The rigid stick approach (Lagrange multiplier formulation) characterized by an infinite tangential contact stiffness converged always but slowly. The reason for latter is that the presence of rigid constraints tends to slow convergence of the Newton solution scheme used in the FE code [2].
The elastic-sticking approach combines the advantages of both evolution rule and rigid-sticking approach. It offers a sufficiently exact approximation of the friction relation at a good convergence rate without additional Lagrange multipliers.

5 Results

All diagrams used in this section show the dynamic behaviour of disc and pin in direction of the normal vector to the disc.

5.1 Experimental results

The experimental part is carried out using the test equipment shown in Figure 1. The test conditions are as follows:

- beam lenght: 151.5 mm (according to a second beam eigenfrequency of 2100 Hz
- rotation speed: 2.4 RPM (according to an average disc velocity of 40 mm/s)
- contact angle: 4° (between normal vector to the disc and neutral axis of the beam)
- normal load: 1.5 kg

Figure 9 shows an example of a "classical" mode lock-in where the spectrum contains a dominant frequency and all of its harmonics.

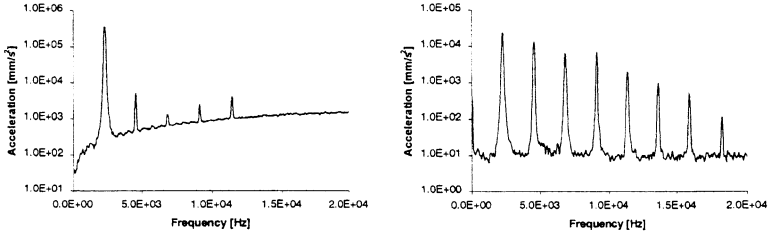

Figure 9. Spectrum from lock-in response for disc (on the left) and beam (on the right)

The lock-in frequency is determined by the third eigenfrequency of the disc (2250 Hz). However the experimental data show, that lock-in does not occur at exactly that frequency, but at a slightly lower one (2215 Hz). In contrast to the spectrum of the beam, which contains five harmonics, the frequency response of the disc shows four harmonics only in the frequency range considered. Furthermore, one can observe that the amplitudes of the beam harmonics decrease monotonically, whereas the amplitudes of the disc harmonics show a completely different behaviour. To verify the results described above, squealing generated during mode lock-in (Figure 10) was measured. The sound spectrum has likewise a dominant frequency and harmonics. This indicates that not only the disc does radiate noise, but the pin as well.

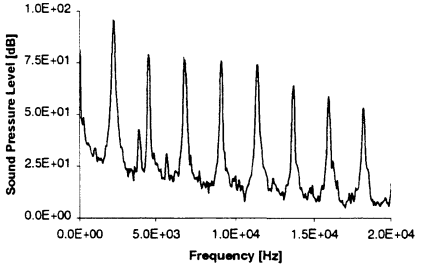

Figure 10. Near field sound spectrum from lock-in response

5.2 Numerical results

In the following section the FE model developed previously is applied to a non-linear time-marching solution. The time step is 4.0E-05 s, corresponding to a frequency range of 0-5 kHz. Before the dynamic analysis is carried out, a static analysis is made in order to bring pin and disc into contact. Rotation speed, contact angle and normal load are equal to the values used in the experimental part whereas beam lenght is varied for generating different eigenfrequencies of the pin.

5.2.1 Friction induced vibrations

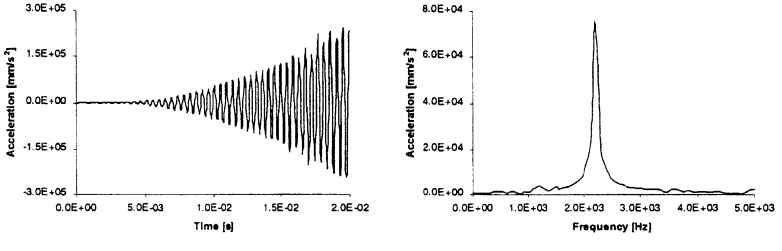

Figure 11. Onset of friction-induced vibrations in time and frequency domain

The main objective in the first part of the numerical studies is to generate friction-induced vibrations. For that purpose, the second eigenfrequency of the beam is trimmed to the same value as the eigenfrequency of the third mode of

the disc. For example, Figure 11 presents a history plot of the out-of-plane acceleration of the disc obtained for the parameters described in section 5.1. It is evident that the oscillations of the system are actually friction-induced and self-excited. They grow as a function of time. By means of a FFT it can be shown that the system does vibrate at almost exactly the third eigenfrequency of the disc and the second eigenfrequency of the beam respectively (2210 Hz).

5.2.2 Mode lock-in

The second part of the numerical investigations deals with mode lock-in. From the experimental section we do know that mode lock-in occurs for example if the second mode of the beam is equal to a frequency of 2100 Hz. Figures 12 and 13 depict the simulation results if mode lock-in takes place. The onset of self-excited oscillations can be observed again. Both pin and disc do vibrate at the same frequency, although the natural frequencies of the both sub-systems do not match (Δf=150 Hz). The dominant frequency in that case is determined by the third natural frequency of the disc. Furthermore, FFT shows that lock-in takes place at a frequency (2197 Hz) which is slightly lower than the eigenfrequency of the disc (2250 Hz). The experimental verification of these results is going to be an issue of future work.

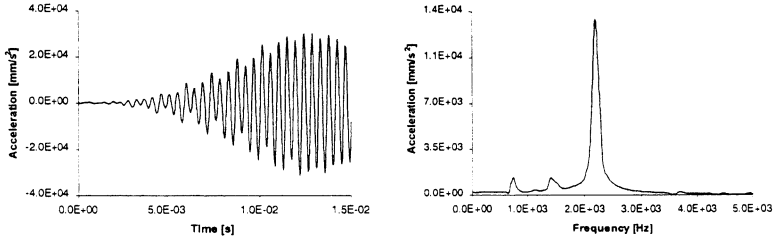

Figure 12. Disc response in time and frequency domain (2197 Hz)

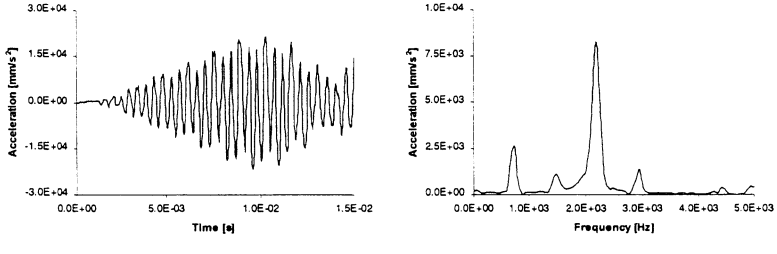

Figure 13. Beam response in time and frequency domain (2197 Hz)

5.2.3 Further numerical example

A further numerical example using a beam lenght of 181.5 mm, corresponding to a second natural frequency of 1500 Hz, is computed in order to show that rather different lock-in conditions can be observed in the numerical study. Figures 14 and 15 show that the model is in a completely different condition, now. Both parts do oscillate at the same frequency but this time the dominant frequency is determined by the beam. This means that the disc is forced to vibrate at almost a

natural frequency of the beam. The look-in frequency (1445 Hz) is likewise slightly smaller again than the eigenfrequency of the beam (1500 Hz).

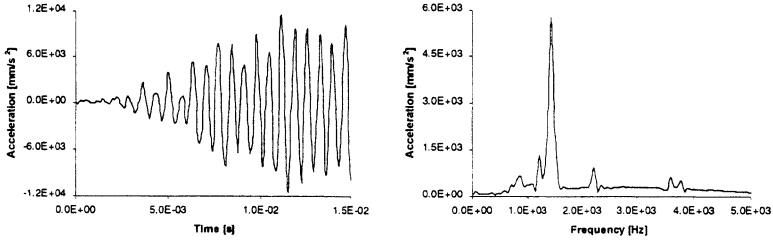

Figure 14. Disc response in time and frequency domain (1445 Hz)

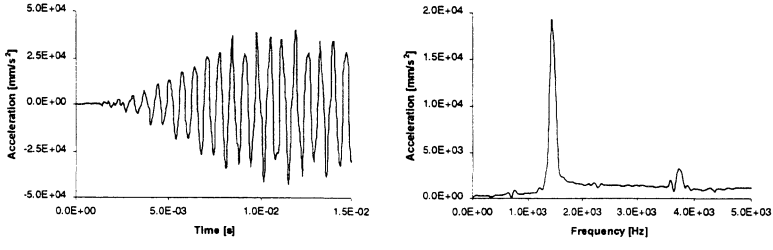

Figure 15. Beam response in time and frequency domain (1445 Hz)

6 Conclusion

In this paper, an experimental and numerical study of the mode lock-in phenomenon, in particular of self-excited friction-induced oscillations was presented. A finite element model of the rotor-stator system, updated by means of experimental modal analysis was used to compute the dynamic behaviour of the experimental set-up if mode lock-in occurs. Extensive numerical studies showed that the elastic-sticking approach based on the penalty method is the most suitable way in that case to introduce friction into a FE code. This approach did reflect the non-linear constitutive friction law, found by using a statistical model based on surface roughness measurements, very well. Furthermore it had a good convergence rate. The numerical predictions for a "classical" mode lock-in case were compared with experimental results. A good correlation was found concerning the look-in frequency. However, the harmonics of the lock-in frequency experimentally observed were not established. By means of a changed beam lenght another situation was investigated purely numerically, where the disc was forced by the pin to oscillate at a frequency determined by the beam.
Modelling friction-induced vibrations using the finite element method provides an analysis tool to obtain a deeper insight into the mechanisms of self-excited oscillations and guidance in avoiding them in the design of sliding systems. Although the model analyzed was relatively simple, the observations and methods used in this work can be applied to the analysis of more complex systems, for example disc brakes.

References

1. Akay, A., Wickert, J. & Xu, Z. *Investigating criteria for the onset of mode lock-in*, Pittsburgh, Carnegie Mellon University, Internal report, 1998.

2. Hibbitt, Karlson & Sorensen, Abaqus Theory Manual 5.8, HKS, Inc., Pawtucket, pp. 5.2.3.1-5.2.3.7, 1998.

3. Laursen, T. A. & Simon, J. C. Continuum-based finite element formulation for the implizit solution of multibody, large deformation frictional contact problems, *Int. J. Num. Meth. Engg.*, 1993, 36, 3451-3485.

4. Willner, K. & Gaul, L. A penalty approach for contact description by FEM based on interface physics, Contact Mechanics II (eds M. H. Aliabadi & C. Alessandri), pp. 257-264, *Proceedings of the 2nd International Conference on Computational Methods in Contact Mechanics*, CMP, Southampton, 1995.